Ryszard STRZELECKI(1), Dmitri VINNIKOV(2)

Electrotechnical Institute/Gdynia Maritime Academy (1)
Tallinn University of Technology (2)

Models of the qZ-Converters

Abstract. **This paper presents** *enhanced* **static and small signal dynamic models of the unconventional qZ-converters family. Static models give consideration to impact of additional** *non shoot-through mode* **with zero current separation diode, occurring in case of weak load current, and losses in dissipative components of the converter. Small signal dynamic models of the qZ-converter allow to immediately evaluate the impact of its elements on control process. Presented here dependencies and results become helpful when designing qZ-converters that work in wide load change interval as well as when designing their controllers.**

Streszczenie. *W* **artykule przedstawiono rozszerzone modele statyczne oraz małosygnałowy model dynamiczny niekonwencjonalnych przekształtników typu qZ. Modele statyczne uwzględniają zarówno tryb pracy z impulsowym prądem diody separującej w stanie aktywnym, występującym w przypadku małych obciążeń, jak również straty w poszczególnych elementach przekształtnika. Model małosygnałowy pozwala ocenić wpływ tych elementów na proces sterowania. Przedstawione wyniki są pomocne przy projektowaniu qZ- przekształtników działających w szerokim zakresie zmian obciążenia oraz równiez projektowaniu ich sterowników (**Modele przekształtników typu qZ**).**

Keywords: Power electronics, DC/AC converter, qZ-converters, impedance input network
Słowa kluczowe: Energoelektronika, przekształtniki DC/AC, przekształtniki typu qZ, wejściowy obwód impedancyjny

Introduction

Inverters with variable voltage that have an input from a low voltage DC source (eg., a PV battery) are mostly realized on the basis of three topologies: a) PWM VSI + DC/DC boost converter without transformer; b) PWM VSI + DC/DC converter with transformer; c) PWM CSI. None of these solutions is fully satisfactory. A more interesting solution is a Z-source converter (ZSC) [1],[2]. The distinguishing feature of this inverter is its input *LC* lattice network [3]. The ZSC circuit provides the single-stage voltage Buck-Boost operation.

Classic ZSC circuit, however, characterizes with impulse input current. This is inadmissible for many sources and in such cases application of large input filters is necessary. To a large extent this shortcoming is avoided in qZ-converter [4], synthesized as a result of transformation of ZCS circuit topology (Figure1). Based on such transformation one should notice the presence of input choke in the qZ-converter. The input choke buffers source current. Moreover, voltage in one of the input circuits is lower than in case of ZSC topology. It is also possible to develop joint earthing of the power source and a bus of transistorized mode. It is also easier to implement multilevel arrangements (especially three-level) cascade systems, which allow to increase voltage conversion ratio [5]. The above indicated characteristics draw more and more attention to qZ-converter systems and non-trivial solutions of input *LC* lattice network [3],[5].

This paper outlines the most significant problems in enhanced static and small signal dynamic models of the qZ-converters family. These models as well as their application are very important at the stage of designing and calculating their elements.

Fundamentals of Static Models

Figure 2 illustrates the equivalent circuits of the qZ-converter for particular modes. Also, based on the circuits static characteristics for all working conditions can be easily derived. For this purpose, in order to simplify mathematic record but at the same time to maintain universality of the proposed ideas, one can assume that:

$$C_1 = C_2\,; \quad L_1 = L_2$$

Even then, the qZ-converter becomes unsymmetrical. Thus:

$$u_{L1} \neq u_{L2} \quad ; \quad u_{C1} \neq u_{C2}$$

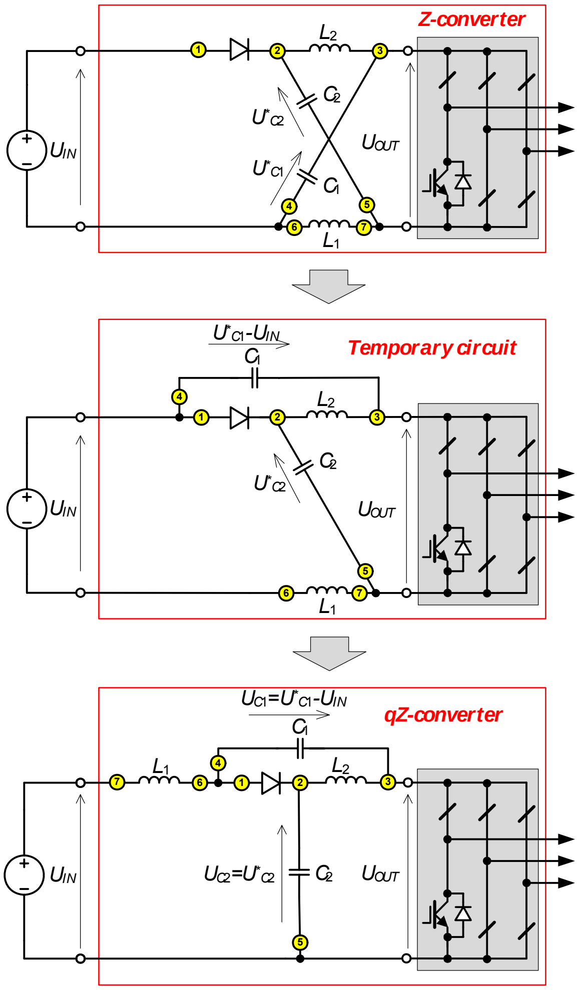

Fig.1. Topological transformation from the Z-converter to qZ-converter

and assumed voltages:

$u_{C1} = U_{C1} = \text{const}$; $u_{C2} = U_{C2} = \text{const}$; $U_0 = \text{const}$

When the converter is in the shoot-through zero state for an interval (t_0, t_1) of the length T_0, during a switching cycle T. From the equivalent circuit (Figure 2a):

$$u_{L1} = U_{C1} + U_{IN} \ ; \ u_{L2} = U_{C2} \ ; \ u_{OUT} = 0$$

When the converter is in the first active state for an interval (t_1, t_2) of the length T_1 (when D-diode is conducting), during a switching cycle T. From the equivalent circuit (Figure 2b):

$$u_{L1} = -U_{C2} + U_{IN} \ ; \ u_{L2} = -U_{C1} \ ; \ u_{OUT} = U_{C1} + U_{C2}$$

When the converter is in the second active state for an interval (t_2, t_0+T) of the length T_2 (when D-diode is not conducting), during a switching cycle T. From the equivalent circuit (Figure 2c):

$$u_{L1} = 0 \ , \ u_{L2} = 0 \ ; \ u_{OUT} = U_{C2} = U_0 \ .$$

Based on the above dependencies and average voltages in cycle T

$$U_{L1} = \int_t^{t+T} u_{L1} dt = 0 \ ; \quad U_{L2} = \int_t^{t+T} u_{L2} dt = 0$$

one obtains:

$$U_{L1} = T_0 \left(U_{C1} + U_{IN} \right) + T_1 \left(U_{IN} - U_{C2} \right) = 0$$

$$U_{L2} = T_0 U_{C2} - T_1 U_{C1} = 0$$

Hence, below dependency is true:

$$U_{C1} = U_{C2} - U_{IN}$$

and:

(1) $$T_1 = \frac{U_{C2}}{U_{C1}} T_0 = \frac{U_{C1} + U_{IN}}{U_{C1}} T_0 = \frac{U_{C2}}{U_{C2} - U_{IN}} T_0$$

In the case of a circuit with no active stages, that is when T_2=0, then if we take into consideration that T_0+T_1=T :

(2a) $$U_{C2} = U_0 = \frac{1 - D_0}{1 - 2D_0} U_{IN}$$

and

(2b) $$u_{OUT(\max)} = U_{C2} + U_{C1} = 2U_{C2} - U_{IN} = \frac{1}{1 - 2D_0}$$

where: D_0=T_0/T - shoot-through coefficient.

Static Models in DCM

The analysis of qZ-converter with small loads and relatively low switching frequency and small inductance L requires more careful approach. With such parameters the converter is working in discontinuous conduction mode (DCM). In this case one must determine moment t_2 or length T_2 of the interval (t_2, t_0+T) when the diode stops to conduct (Figure 3). After deriving T_2 or coefficient $D_2=T_2/T$ and transformation (1) one receives:

(3a)
$$U_{C2} = U_0 = \frac{1 - D_0 - D_2}{1 - 2D_0 - D_2} U_{IN}$$

and

(3b)
$$u_{OUT(\max)} = U_{C2} + U_{C1} = \frac{1 - D_2}{1 - 2D_0 - D_2} U_{IN}$$

Equations (3a) and (3b) illustrates also that transition from continuous conduction mode (CCM) to DCM increases output voltage. This effect can lead to destabilized work and work failure. One should note that DCM occurs only when currents $i_{L1}=i_{L2}$ in chokes $L_1=L_2$ decrease to ½I_0 in the interval (t_1, t_0+T). From this moment till the end of switching cycle currents $i_{L1}=i_{L2}=$½I_0. In universal case, when $L_1 \neq L_2$ to $i_{L1}+i_{L2}=I_0$.

a) shoot-through mode (duration T_0)

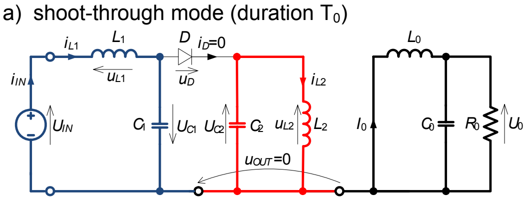

b) non shoot-through mode when $i_D>0$ (duration T_1)

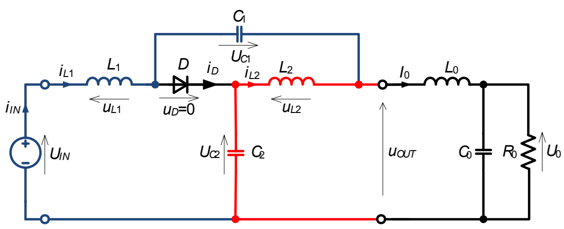

c) non shoot-through mode when $i_D=0$ (duration T_2)

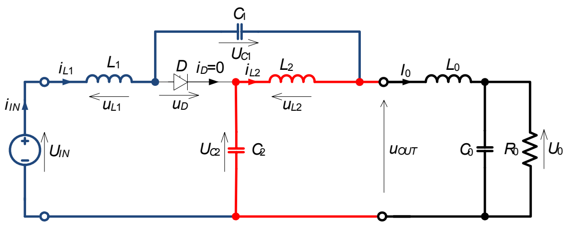

Fig.2. Operation modes of the qZ-converter in the switching period T= $T_0+T_1+T_2$

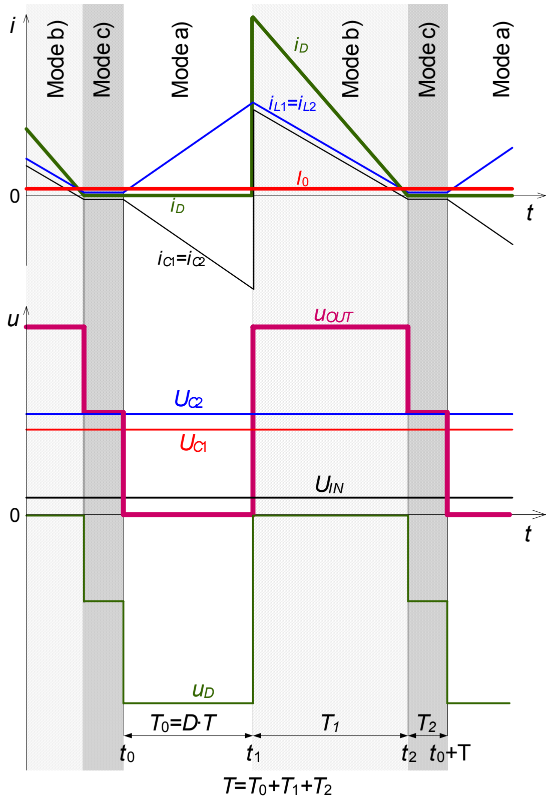

Fig.3. Voltages and currents of the qZ-converter in the switching period T= $T_0+T_1+T_2$

In order to define the impact that parameters have on the converter DCM, one should determine average value of I_L current $i_{L1}=i_{L2}$. Based on equivalent circuit diagram (Figure 2) and shape of runs presented on figure 3, and dependencies (1), one obtains:

(4) $$I_L = \frac{I_0}{2} + \frac{U_0 T_1}{2L}\left(T_0 + T_1\right) = \frac{I_0}{2} + \frac{U_0 D_0^2}{2Lf}\left(\frac{2U_0 - U_{IN}}{U_0 - U_{IN}}\right)$$

where f=1/T – switching frequency.

Taking into account the above equation and balance of input active power P_{IN} and output P_0:

$$P_{IN} = I_L U_{IN} = I_0 V_0 = P_0$$

One can record:

(5) $$\frac{1 + U_0/\left(U_0 - U_{IN}\right)}{1 - U_{IN}/2U_0} D_0^2 = \frac{2 I_0 L f}{U_{IN}}$$

Then, introducing the coefficient

(6) $$\gamma = 2I_0Lf/U_{IN}$$

Characteristic of voltage conversion ratio qZ-converter in DCM can be expressed by equation:

(7) $$U_0 = \frac{\gamma}{\gamma - 2D_0^2}U_{IN}$$

Comparing dependencies (2) and (7) an including (6) we can also define Basic parameters of qZ-converter, where no DCM occurs. These parameters are defined by equation:

$$L > \left(D_0 - D_0^2\right)U_{IN}/I_0 f$$

Figure 4 illustrates characteristics of voltage conversion ratio in *γ* parameter function for various values of shoot-through coefficient D_0. It is not difficult to notice that in the DCM area the output voltage is elevated. Moreover, based on the equation (7), with regards to stability, operation close to the coefficient value is inadmissible:

$\gamma < 2D_0^2$ or, considering the formula (6), $D_0 > \sqrt{I_0Lf/U_{IN}}$

It is advisible to control one of the dependencies in the control system.

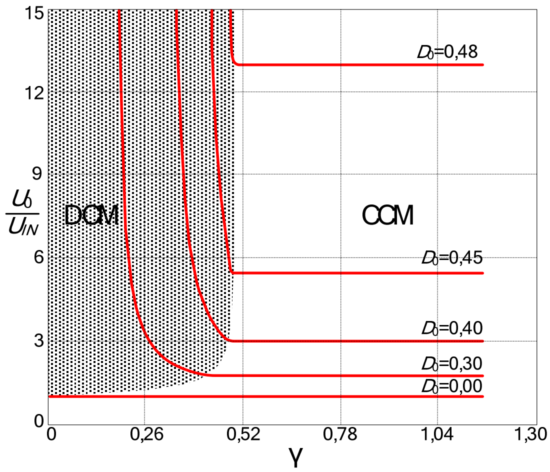

Fig.4. Voltage conversion ratio, including CCM and DCM

Static Model with Losses

The information demonstrated above relate only to loss-less qZ-converter, and therefore evaluation of practical implementation of the arrangement is more difficult.

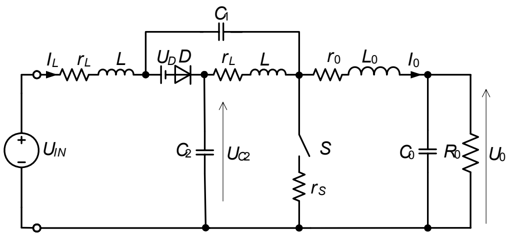

Fig.5.Simple equivalent qZ-converter circuit with take into account losses

Figure 5 demonstrates simple equivalent diagram of qZ-converter with consideration given to losses in chokes and coupler S, controlled by resistances , and losses in D-diode controlled by voltage drop in the diode U_D in the conducting state. Taking this arrangement into consideration and following the procedures similar to those in the previous chapter, for CCM one receives the following equations:

$$U_0 = \frac{\dfrac{\left[D_0\left(r_L + 2r_S\right) + r_L\left(1 - D\right)D_0\right]}{r_S D_0 I_0 + \left(1 - D_0\right)\left(U_D - U_{IN}\right)} I_L - 1}{\dfrac{2D_0 - 1}{r_S D_0 I_0 + \left(1 - D_0\right)\left(U_D - U_{IN}\right)}}$$

$$I_0 = \frac{\left(1 - D_0\right)\left(2U_0 + U_D - U_{IN}\right) + 2r_S D_0 I_L}{D_0\left(R_0 + r_0 + r_S\right) + \left(R_0 + r_0\right)\left(1 - D_0\right)}$$

$$I_L = I_0\left(1 - D_0\right) / \left(1 - 2D_0\right)$$

On the basis of these dependencies, after simple arithmetic conversions, the dependency describing output voltage in the function of shoot-through coefficient D_0 takes:

$$U_0 = \frac{\dfrac{\left(U_D - U_{IN}\right)\left(-2D_0^2 + 3D_0 - 1\right)R_0}{r_L\left(2D_0^2 - 4D_0 + 2\right) + r_S D_0}}{\dfrac{\left(R_0 + r_0\right)\left(4D_0^2 - 4D_0 + 1\right)}{r_L\left(2D_0^2 - 4D_0 + 2\right) + r_S D_0} + 1} \tag{8}$$

while

$$if \quad \left\{\begin{array}{l} r_L \to 0 \\ r_0 \to 0 \\ r_S \to 0 \\ U_D \to 0 \end{array}\right\} \quad then \quad U_0 \to U_{C2} \to \frac{1 - D_0}{1 - 2D_0} U_{IN}$$

Dependency (8) derived for parameters:

$$U_{IN} = 30\text{V} \quad R_0 = 3\Omega \quad r_L = 11\text{m}\Omega$$
$$r_0 = 12\text{m}\Omega \quad r_S = 30\text{m}\Omega \quad V_D = 1\text{V} \;,$$

close to those in reality and the dependency (2), are presented on figure 6. The comparison leads to a conclusion that in practice one must take into account maximum voltage conversion ratio $U_0/U_{IN} \leq 3 \div 4$.

Loss-less Dynamic Model

Figure 7 illustrates tested dynamic model of the qZ-converter, which regards CCM, and in which the *D*-diode (Figure 2) was replaced with switch NOT(*S*), synchronized with the switch *S*.

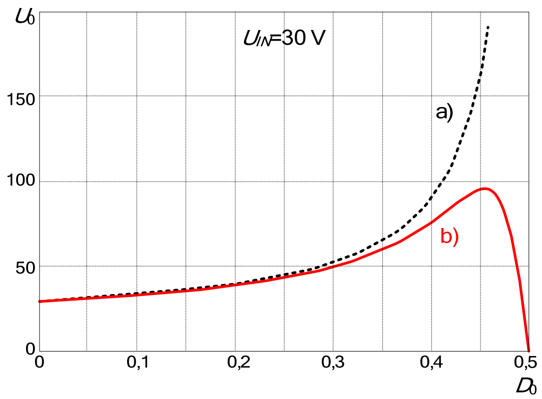

Fig.6. Output voltage vs. duty cycle D_0 for qZ-converter without (a) and with (b) losses

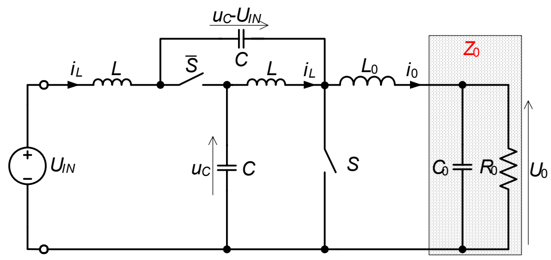

Fig.7. Testing dynamic model of the qZ-converter

This model is described by the following differential equations:
- in shoot-through state (intervals of length $D_0 \cdot T$)

$$\begin{bmatrix} L\dfrac{di_L}{dt} \\ C\dfrac{du_C}{dt} \\ L_0\dfrac{di_0}{dt} \end{bmatrix} = \underbrace{\begin{bmatrix} 0 & 1 & 0 \\ -1 & 0 & 0 \\ 0 & 0 & -Z_0 \end{bmatrix}}_{A_1} \cdot \underbrace{\begin{bmatrix} i_L \\ u_C \\ i_0 \end{bmatrix}}_{X} + \underbrace{\begin{bmatrix} 0 \\ 0 \\ 0 \end{bmatrix}}_{B_1} \cdot U \qquad (9)$$

- in active state (intervals of lenght $D_1 \cdot T$)

(10)
$$\begin{bmatrix} L\dfrac{di_L}{dt} \\ C\dfrac{du_C}{dt} \\ L_0\dfrac{di_0}{dt} \end{bmatrix} = \underbrace{\begin{bmatrix} 0 & -1 & 0 \\ 1 & 0 & -1 \\ 0 & 2 & -Z_0 \end{bmatrix}}_{A_2} \cdot \underbrace{\begin{bmatrix} i_L \\ u_C \\ i_0 \end{bmatrix}}_{X} + \underbrace{\begin{bmatrix} 1 \\ 0 \\ -1 \end{bmatrix}}_{B_2} \cdot U$$

where $U=U_{IN}$, and also $D_0+D_1=1$ (since CCM is under consideration).

At the same time [6] it is known, that equations describing a model of the converter:

$$K\frac{d}{dt}X = A_1X + B_1U \quad \text{in interval } T_0 \text{ when } S=1$$

$$K\frac{d}{dt}X = A_2X + B_2U \quad \text{in interval } T_1 \text{ when } S=0$$

can be recorded for small gains as:

$$K\frac{d}{dt}\tilde{X} = A\tilde{x} + B\tilde{u} + \left[\left(A_1 - A_2\right)X + \left(B_1 - B_2\right)U\right] \cdot \tilde{d}$$

where: $B = B_1 \cdot D_0 + B_2 \cdot D_1$; $A = A_1 \cdot D_0 + A_2 \cdot D_1$

Hence, taking into consideration matrixes A_1, A_2, B_1, B_2 included in the equations (9) and (10) as well as the fact that in the case of CCM one has $D_1=1-D_0$, one obtains:

(11)
$$\begin{bmatrix} L\dfrac{d\tilde{i}_L}{dt} \\ C\dfrac{d\tilde{u}_C}{dt} \\ L_0\dfrac{d\tilde{i}_0}{dt} \end{bmatrix} = \begin{bmatrix} 0 & 2D_0-1 & 0 \\ 1-2D_0 & 0 & D_0-1 \\ 0 & 2-2D_0 & -Z_0 \end{bmatrix} \cdot \begin{bmatrix} \tilde{i}_L \\ \tilde{u}_C \\ \tilde{i}_0 \end{bmatrix} + \\ + \begin{bmatrix} 1-D_0 \\ 0 \\ D_0-1 \end{bmatrix} \cdot \tilde{u}_{IN} + \begin{bmatrix} 2U_C - U_{IN} \\ -2I_L + I_0 \\ -2U_C + U_{IN} \end{bmatrix} \cdot \tilde{d}$$

Further, by applying Laplace transformation to the (11), one can write:

(12a)
$$sL \cdot \tilde{i}_L(s) = \left(2D_0 - 1\right) \cdot \tilde{u}_c(s) + \left(1 - D_0\right) \cdot \tilde{u}_{IN}(s) + \\ + \left(2U_C - U_{IN}\right) \cdot \tilde{d}(s)$$

(12b)
$$sC \cdot \tilde{u}_C(s) = \left(1 - 2D_0\right) \cdot \tilde{i}_L(s) + \left(D_0 - 1\right) \cdot \tilde{i}_0 + \\ + \left(-2I_L + I_0\right) \cdot \tilde{d}(s)$$

(12c) $sL_0 \cdot \tilde{i}_0(s) = (2-2D_0)\cdot \tilde{u}_c(s) - Z_0(s)\cdot \tilde{i}_0(s) + (D_0-1)\cdot \tilde{u}_{IN}(s) - (2U_C - U_{IN})\cdot \tilde{d}(s)$

On the basis of derived dependencies (12) it is easy determine appropriate transfer functions. For example one can assume that load Z_0 at working point (I_0, U_{IN}, U_C, D_0, I_L) and gains:

$$\tilde{i}_L(s) = 0 \;\; ; \;\; \tilde{u}_c(s) = 0 \;\; ; \;\; \tilde{u}_{IN} = 0 \, ,$$

one can evaluate dynamics of changes in output voltage qZ-converter with changes duty cycle $D_0 \pm \tilde{d}$. Transfer function describes this dynamic in case where:

$$Z_0(s) = R_0 / (C_0 R_0 s + 1)$$

is as follows:

(13) $$\tilde{u}_0(s) / \tilde{d}(s) = L(s) / M(s)$$

where:

$$L(s) = R_0 U_{IN} + [2R_0 L(D_0 - 1)(2I_L - I_0)]\, s + \\ + [R_0 LC(U_{IN} - 2U_C)] s^2$$

$$M(s) = \{L_0 LCC_0 R_0\} s^4 + \{L_0 LC\} s^3 \\ + \left\{ \begin{matrix} LR_0 \left[2C_0 \left(1 + D_0^2 - 2D_0\right) + C \right] + \\ L_0 C_0 R_0 \left(4D_0^2 - 4D_0 + 1\right) \end{matrix} \right\} s^2 \\ + \left\{ L_0 \left(1 - 4D_0 + D_0^2\right) + 2L\left(1 - 2D_0 + D_0^2\right) \right\} s \\ + R_0 \left\{1 - 4D_0 + 4D_0^2\right\}$$

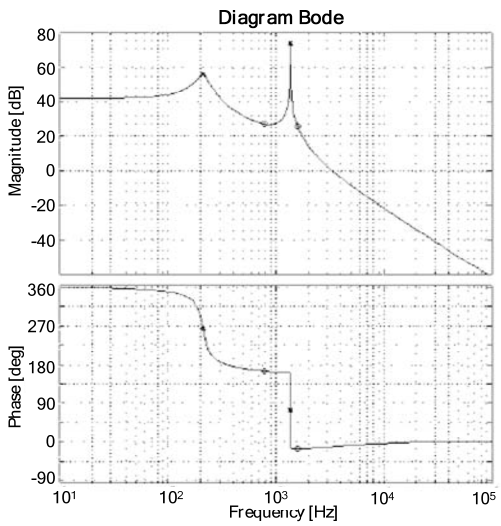

Fig.8. Diagram Bode of the testing dynamic model of the qZ-converter.

Figure 8 presents diagram Bode determined on the basis of the equation (13). Run of the diagram for higher frequency draws attention as it indicates the need of careful selection of settings in order to assure stability of the arrangement and high control dynamics, without oscillations and need for significant readjustment.

Conclusions

Simulations results confirm the theoretically results of the paper. However, no experiments under conditions comparable to theoretical model were conducted. According to authors, the results of simulation should be correct as they are confirmed in designing the laboratory model of qZ-converter. First of all, the presented results were used to select control settings and the main circuit parameters, so that DCM does not occur.

In the laboratory model, under normal operational conditions of CCM, maximum achieved voltage conversion ratio was slightly higher than 3,5. This indicates that the quantitative characteristics of the effect of real losses of the converter's components on its static parameters were well recognized.

One should also note that start-up processes of the converter without feedback characterized with large oscillations and long transient process, which is also confirmed by bode diagram.

One of the important future steps with regards to the project is the frequency analysis of a qZ-converters in a close circuit for different controllers. Further research will be directed toward more detailed inclusion of losses at both static and dynamic states.

This work was financed by the Polish Ministry of Science and Higher Education (2009–2011)

REFERENCES

1. Peng F.Z., Z-Source Inverter, *IEEE Trans. on Ind. Applications*, 39 (2003), n.2, 504-510
2. Strzelecki R., Wojciechowski D., Adamowicz M., Wilk A., Mosoń I., Three-phase NPC Z-source inverter, *Electrotechnical Review*, 82(2006), nr.10, 54-60
3. Strzelecki R., Bury W., Adamowicz M., Strzelecka N., New Alternative Passive Networks to Improve the Range Output Voltage Regulation of the PWM Inverters. *Proc. of the APEC'09*, 2009, 857- 863
4. Anderson J., Peng F.Z., Four Quasi-Z-Source Inverters, *Proc of the PESC'08*, 2008, 2743-2749
5. Strzelecki R., Adamowicz M., Przekształtniki podwyższająco- obniżające DC-AC z kaskadowymi obwodami typu qZ, *Materiały Konferencji SENE'09*, CD-ROM, 2009
6. Ericson R.W., Maksimovic D., Fundamentals of Power Electronics, *Kluwer Academic Publishers*, 2001

***Autorzy**: Prof. Ryszard Strzelecki, Electrotechnical Institute, 28 Pożaryskiego str., 04-703 Warsaw (Gdynia Maritime Academy, 81-87 Morska str., 81-225 Gdynia), E-mail: rstrzele@am.gdynia.pl; D.Sc. Dmitri Vinnikov, Senior Researcher, Tallinn University of Technology, 5 Ehitajate str., 19086 Tallinn, E-mail: dm.vin@mail.ee*